Ocean Surface Wave Optical Roughness: Innovative Polarization Measurement

Christopher J. Zappa
Lamont-Doherty Earth Observatory of Columbia University
Ocean and Climate Physics Division
61 Route 9W
Palisades, NY 10964
phone: (845) 365-8547 fax: (845) 365-8157 email: zappa@ldeo.columbia.edu

Award Number: N00014-06-1-0372

LONG-TERM GOALS

We are part of a multi-institutional research team funded by the ONR-sponsored Radiance in a Dynamic Ocean (RaDyO) program. The primary research goals of the program are to (1) examine time-dependent oceanic radiance distribution in relation to dynamic surface boundary layer (SBL) processes; (2) construct a radiance-based SBL model; (3) validate the model with field observations; and (4) investigate the feasibility of inverting the model to yield SBL conditions. The goals of our team are to contribute innovative measurements, analyses and models of the sea surface roughness at length scales as small as a millimeter. This characterization includes microscale and whitecap breaking waves.

The member of the research team are:

Michael Banner, School of Mathematics, UNSW, Sydney, Australia

Johannes Gemmrich, Physics and Astronomy, UVic, Victoria, Canada

Russel Morison, School of Mathematics, UNSW, Sydney, Australia

Howard Schultz, Computer Vision Laboratory, Computer Science Dept, U. Mass., MA

Christopher J Zappa, Lamont Doherty Earth Observatory, Palisades, NY

OBJECTIVES

Nonlinear interfacial roughness elements - sharp crested waves, breaking waves as well as the foam, subsurface bubbles and spray they produce, contribute substantially to the distortion of the optical transmission through the air-sea interface. These common surface roughness features occur on a wide range of length scales, from the dominant sea state down to capillary waves. Wave breaking signatures range from large whitecaps with their residual passive foam, down to the ubiquitous centimeter scale microscale breakers that do not entrain air. There is substantial complexity in the local wind-driven sea surface roughness microstructure, as is evident in the close range image shown in Figure 1. Traditional descriptors of sea surface roughness are scale-integrated statistical properties, such as significant wave

Report Documentation Page

Form Approved
OMB No. 0704-0188

1. REPORT DATE	2. REPORT TYPE	3. DATES COVERED
2010		**00-00-2010 to 00-00-2010**

4. TITLE AND SUBTITLE	5a. CONTRACT NUMBER
Ocean Surface Wave Optical Roughness: Innovative Polarization Measurement	5b. GRANT NUMBER
	5c. PROGRAM ELEMENT NUMBER
6. AUTHOR(S)	5d. PROJECT NUMBER
	5e. TASK NUMBER
	5f. WORK UNIT NUMBER
7. PERFORMING ORGANIZATION NAME(S) AND ADDRESS(ES) **Lamont-Doherty Earth Observatory of Columbia University,Ocean and Climate Physics Division,61 Route 9W,Palisades,NY,10964**	8. PERFORMING ORGANIZATION REPORT NUMBER
9. SPONSORING/MONITORING AGENCY NAME(S) AND ADDRESS(ES)	10. SPONSOR/MONITOR'S ACRONYM(S)
	11. SPONSOR/MONITOR'S REPORT NUMBER(S)

12. DISTRIBUTION/AVAILABILITY STATEMENT
Approved for public release; distribution unlimited

13. SUPPLEMENTARY NOTES

14. ABSTRACT

15. SUBJECT TERMS

16. SECURITY CLASSIFICATION OF:			17. LIMITATION OF ABSTRACT	18. NUMBER OF PAGES	19a. NAME OF RESPONSIBLE PERSON
a. REPORT **unclassified**	b. ABSTRACT **unclassified**	c. THIS PAGE **unclassified**	**Same as Report (SAR)**	**12**	

height, mean squared slope (e.g. Cox and Munk, 1954) and breaking probability (e.g. Holthuijsen and Herbers, 1986). Subsequently, spectral characterisations of wave height, slope and curvature have been measured, providing a scale resolution into Fourier modes for these geometrical sea roughness parameters. More recently, measurements of whitecap crest length spectral density (e.g. Phillips et al, 2001, Gemmrich et al., 2008) and microscale breaker crest length spectral density (e.g. Jessup and Phadnis, 2005) have been reported.

Our effort seeks to provide a more comprehensive description of the physical and optical roughness of the sea surface. We will achieve this through the analysis of our suite of comprehensive sea surface roughness observational measurements within the RADYO field program. These measurements are designed to provide optimal coverage of fundamental optical distortion processes associated with the air-sea interface. In our data analysis, and complementary collaborative effort with RaDyO modelers, we are investigating both spectral and phase-resolved perspectives. These will allow refining the representation of surface wave distortion in present air-sea interfacial optical transmission models.

APPROACH

We build substantially on our accumulated expertise in sea surface processes and air-sea interaction. We are working within the larger team (listed above) measuring and characterizing the surface roughness. The group plans to contribute the following components to the primary sea surface roughness data gathering effort in RaDyO:

- *polarization camera measurements* of the sea surface slope topography, down to capillary wave scales, of an approximately 1m x 1m patch of the sea surface (see Figure 1), captured at video rates. [Schultz, Zappa]
- *co-located and synchronous orthogonal 75 Hz linear scanning laser altimeter* data to provide spatio-temporal properties of the wave height field (resolved to O(0.5m) wavelengths) [Banner, Morison]
- *high resolution video imagery* to record whitecap data, from three cameras, close range and broad field [Gemmrich, Zappa]
- *fast response, infrared imagery* to quantify properties of the microscale breakers, and surface layer kinematics and vorticity [Zappa]
- *air-sea flux package including sonic anemometer* to characterize the near-surface wind speed and wind stress [Zappa]

The team's envisaged data analysis effort includes: detailed analyses of the slope field topography, including mean square slope, skewness and kurtosis; laser altimeter wave height and large scale wave slope data; statistical distributions of whitecap crest length density in different scale bands of propagation speed and similarly for the microscale breakers, as functions of the wind speed/stress and the underlying dominant sea state. Our contributions to the modeling effort will focus on using RaDyO data to refine the sea surface roughness transfer function. This includes the representation of nonlinearity and breaking surface wave effects including bubbles, passive foam, active whitecap cover and spray, as well as micro-breakers.

WORK COMPLETED

Our effort in FY10 has comprised the processing and analysis of the suite of sea surface roughness measurements conducted during the Scripps Institution of Oceanography (SIO) Pier Experiment from January 6-28, 2008, the RaDyO field experiment in the Santa Barbara channel aboard R/P Flip during September 5-27, 2008, and the RaDyO field experiment in the Western Pacific Ocean off Hawaii aboard R/P Flip during 28 August to 16 September, 2009.

In all experiments, from the SIO Pier and from both Flip experiments, we had the responsibility for infrared imagery, visible imagery, laser altimetry, and air-sea fluxes of heat, mass, and momentum as well as radiative fluxes. During FY10, we also refined our data processing and protocols and continued work on analysis techniques for characterizing the various roughness features.

We carried out processing and validation of our infrared/visible and air-sea flux data gathered during each of the 2008 field experiments. These measurements were collocated with our partner investigators' high resolution polarimeteric and optical imaging systems collecting the surface roughness data as well as two lidars mounted in quadrature. We also progressed with our effort to develop a robust 'individual breaker' decomposition capability so that local physical microbreaking elements can be detected and characterized along with their space-time phasing, thereby overcoming the classical Fourier spectrum issue of bound versus free wave contributions in assessing true physical sea surface roughness.

Of major significance to our group's effort was Howard Schultz's successful DURIP application to build a full polarization camera for use in RaDyO. Further details on progress with this development are given in the companion ONR RaDyO Annual Report by Schultz.

In both Flip experiments Howard Schultz had the overall responsibility for the Narrow field-of-view Imaging Polarimeter (N-IPol) instrumentation. Dr. Christopher Zappa installed the N-IPol on FLIP, collected the data, and has been the primary data processor. The data processing and analysis will be a collaborative effort between Howard Schultz, Christopher Zappa, Mike Banner, and Larry Pezzaniti (with Polaris Sensor Technologies).

Figure 1 shows the instrumentation deployed from R/P Flip. Banner/Morison deployed two orthogonal line scanning lidars, synchronized for zero crosstalk. These were positioned on the boom so that their intersection point was within the common footprint of the polarimetric (Schultz), infrared (Zappa) and visible (Gemmrich) imagery cameras to measure small-scale surface roughness features and breaking waves. Zappa deployed his infrared/visible camera system (with blackbody target, a blackbody controller, and laser altimeter). The infrared camera was mounted near the polarimeter and the visible camera was mounted on the end of the boom to collocate the IR, N-IPol, and visible imagery. He also deployed his environmental monitoring system (sonic anemometer, a Licor water vapor sensor, a Vaisala RH/T/P probe, a motion package, a pyranometer, and a pyrgeometer). Gemmrich deployed 2 video visible imagery cameras. One camera was mounted on the main boom next to our other instrumentation packages. The second camera was mounted higher up to provide a wider perspective on larger scale breaking events. Schultz deployed an instrument package located on the boom that includes a polarimetric camera imaging the very small-scale waves. The individual data acquisition systems were synchronized to GPS accuracy which allowed the various data sets to be interrelated to within 0.01 seconds. The IR and N-IPol imagery were triggered at a frame rate of 60 Hz on the same pulse such that their timing synchronization was better than 1 ms. Note that the N-IPol and IR cameras

were offset to account for the difference in nominal incidence angles of 20 for the IR and 35 for the N-IPol.

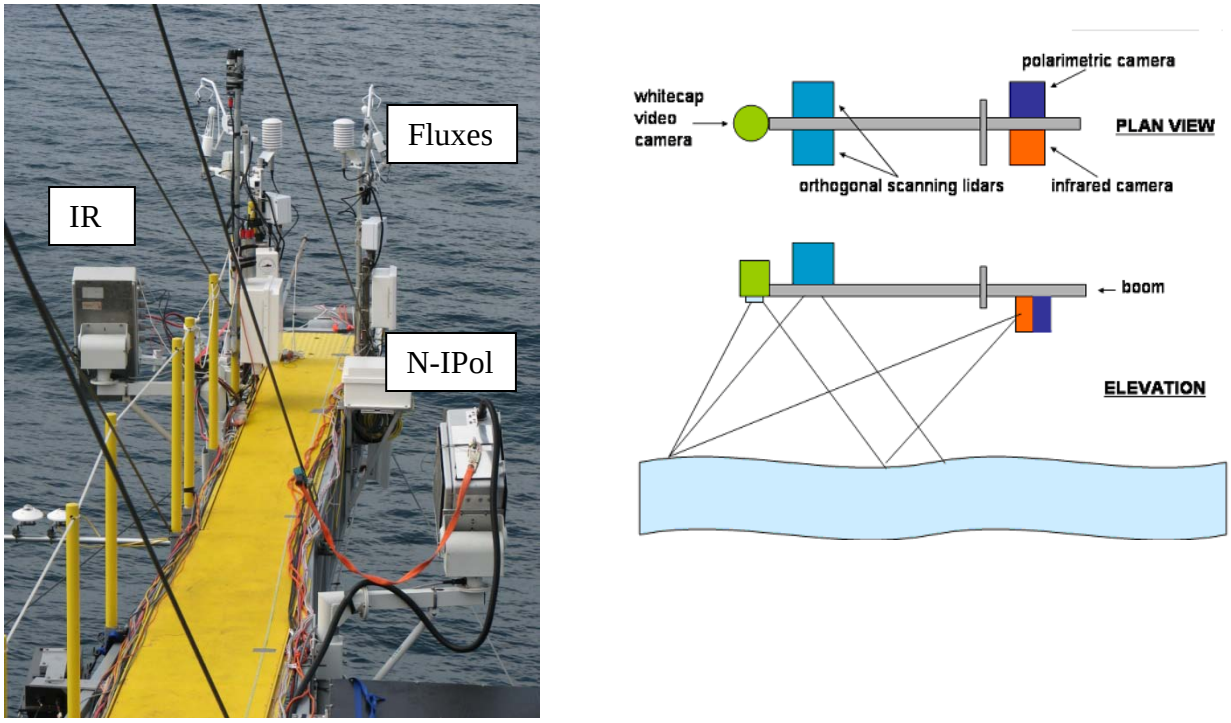

Figure 1. The left panel shows the instrumentation test set-up from the Starboard Boom on FLIP during the RaDyO Santa Barbara Channel Experiment. The right panel shows a schematic of instrumentation packages deployed. The visible camera and laser altimeter are located at the end of the boom and not easily visible in this picture. The boom was about 9m above the mean water level. The incidence angles of the IR, visible, and N-IPol cameras as well as the laser altimeter were such that they viewed an overlayed patch of the water surface directly beneath the end of the boom.

RESULTS

Publication of the first manuscript demonstrating the feasibility of the polarimeteric slope sensing technique was completed. The manuscript was published in Measurement, Science and Technology entitled "Retrieval of short ocean wave slope using polarimetric imaging" [*Zappa et al.*, 2008].

Our complete system was field-deployed from FLIP during the first intensive observational experiment during September 2008 in the Santa Barbara channel. Our systems included infrared/visible imagery, laser altimetry, and air-sea fluxes of heat, mass, and momentum as well as radiative fluxes. A moderate range of sea state conditions prevailed with the wind speed, U_{10}, ranged from light and variable, up to 12 m s^{-1} and the significant wave height ranged from 0.7 m to 2.0 m. Figure 2 below shows a summary of the wind speed and wave heights measured during September 2008. The instruments were deployed from a boom at a height of ~9 m above the mean sea level. The data show a distinctive and persistent diurnal structure to the wind speed that was stronger in the afternoon relative to in the morning. The laser altimeter operated better in the strong wind forcing conditions, as

expected, where the increase in specular surface facets provides more comprehensive return for the time-of-flight measurement. Our experience confirmed that this method will provide useful data on the height of the dominant waves. This information characterizes the background environment experienced by the short wind waves (the sea surface microstructure roughness) measured by the IR and N-IPol imagery.

During August 23-September 16, 2009 off Hawaii in the Western Pacific Ocean, a moderate range of sea state conditions prevailed with the wind speed, U_{10}, steadily decreased from 12 m s^{-1} to and the significant wave height ranged from 1.7 m to 2.7 m. Figure 3 below shows a summary of the wind speed and wave heights measured during September 2008. The instruments were deployed from a boom at a height of ~9 m above the mean sea level. The data show a distinctive decrease in wind speed and a persistent wave energy level that was higher than during Santa Barbara Channel.

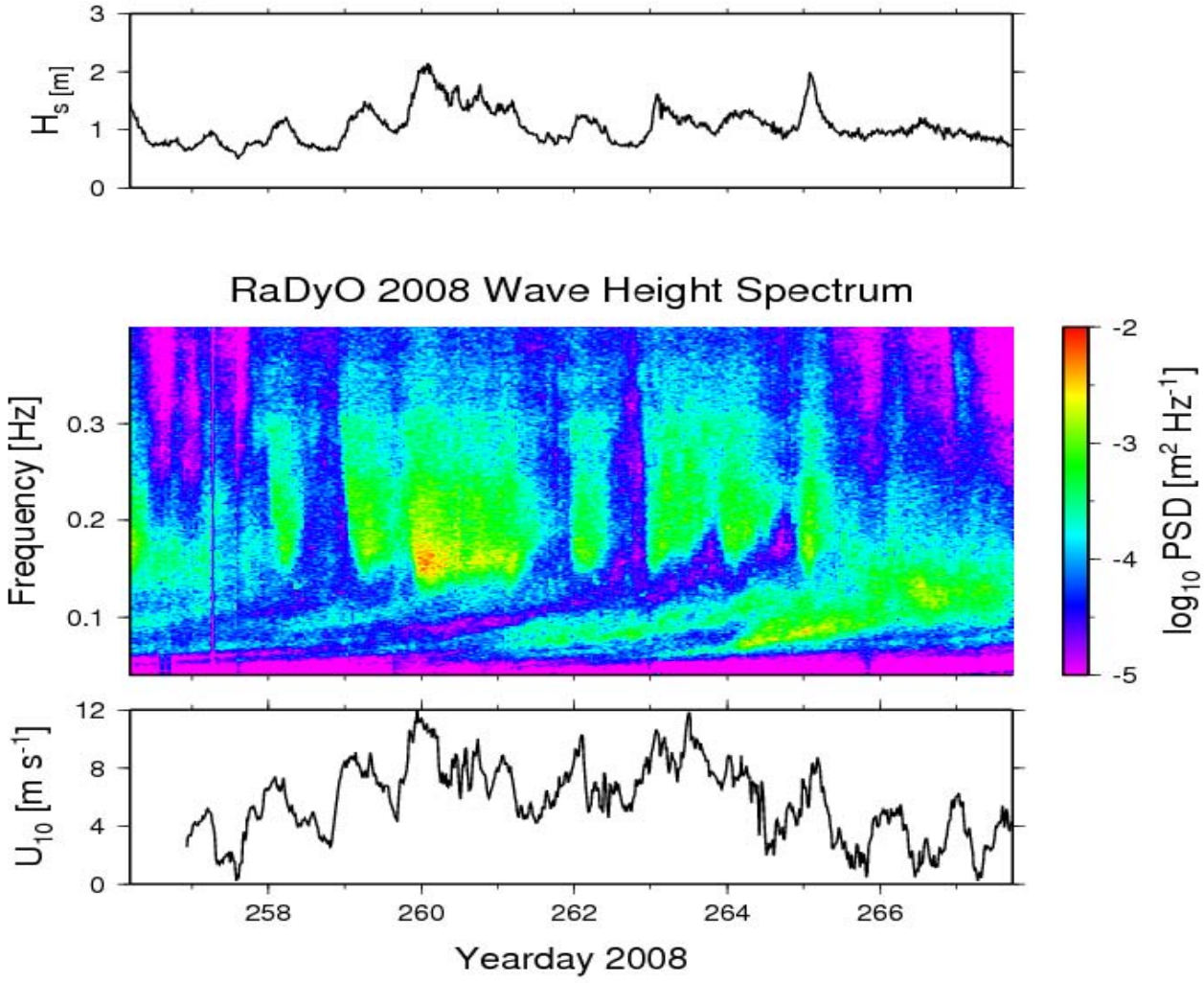

Figure 2. Time series of the wind speed (sonic anemometer), significant wave height (laser altimeter), and wave height frequency spectra during the RaDyO Santa Barbara Channel Experiment aboard the R/P FLIP. The measurements were made from the starboard boom at a nominal height of roughly 9 m.

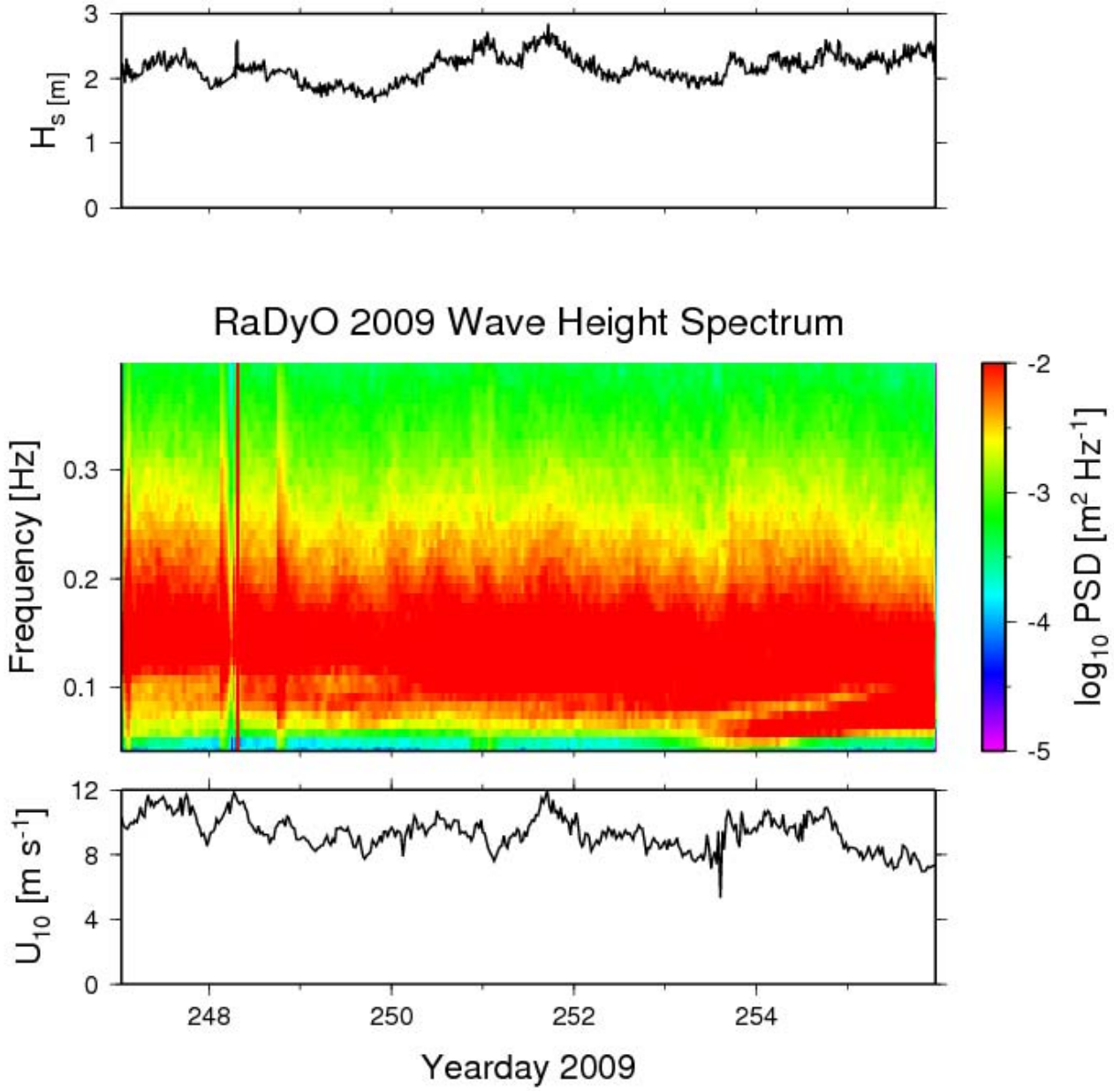

Figure 3. Time series of the wind speed (sonic anemometer), significant wave height (laser altimeter), and wave height frequency spectra during the RaDyO Western Pacific Experiment aboard the R/P FLIP. The measurements were made from the starboard boom at a nominal height of roughly 9 m.

We have calibrated and processed all the Santa Barbara Benign Wind Conditions and Western Pacific polarimetric data. We encountered a significant algorithm development effort, including 1) correcting for fixed pattern noise, and 2) correcting for variable gain between sensors. We were able to recover surface slopes with the new N-IPol instrument and synchronize the Infrared and N-IPol instruments. Figure 4 shows a sample intensity JADE IR image, a high resolution Imperx video image, and x- and

y-slope images from the Polaris N-IPol. There were a few N-IPol calibration issues related to determining the registration and relative sensitivity of the four internal CCD images. These calibration issues were resolved and incorporated into the Santa Barbara channel and Hawaii experimental procedures. We produced time lapsed video of the X and Y Slope images which were shown at the Environmental Optics Program meeting held in Portland, OR February 2010. These slope features are characterized by steep slopes that also have high spatial variance that exhibits a dimpled structure observed previously in the laboratory by *Zappa et al*. [2004].

The N-IPOL has provided useful data on the local directional slope of the gravity waves, and the initial 1-meter baseline slope intercomparison with the Lidar slope shows very close agreement for frequency spectra (Figure 5 Left) of 20 minute records and higher than 0.8 magnitude squared coherence level in the frequency range from 0.3 to 0.8 Hz (Figure 5 Right). In addition, the polarimeter data characterizes the background environment experienced by the very short wind waves that comprise the sea surface microstructure. This information allows accurate phasing of the polarimetric, infrared and visible camera imagery of the sea surface microstructure with respect to the underlying dominant wind waves.

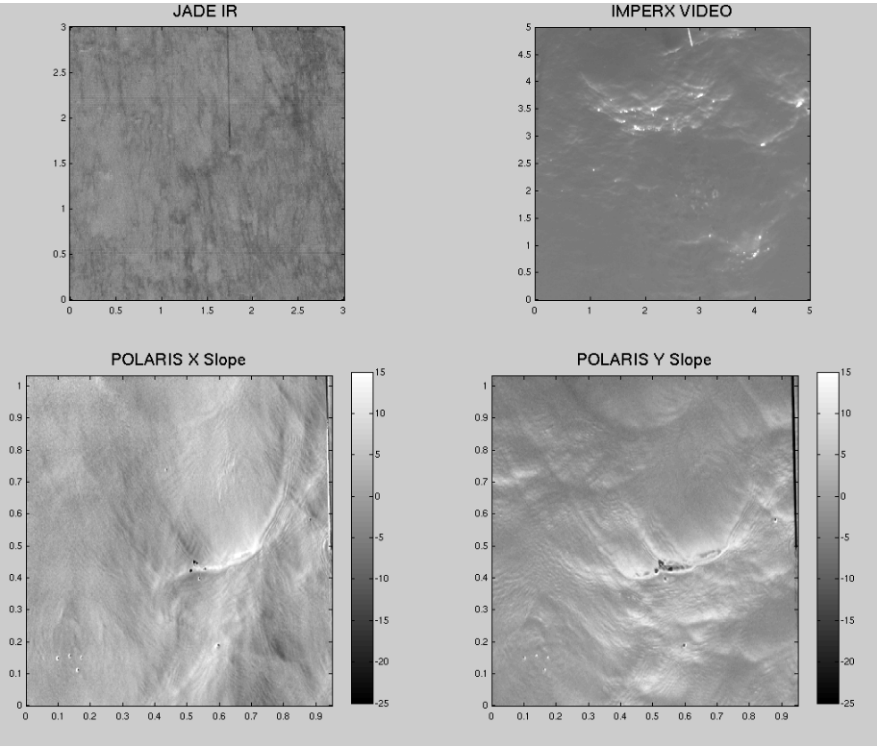

Figure 4. A typical co-located data snapshot show the infrared image (Top Left), a high-resolution video image (Top Right), and the X- (Bottom Left) and Y-Slope (Bottom Right) image during the RaDyO Santa Barbara Channel Experiment.

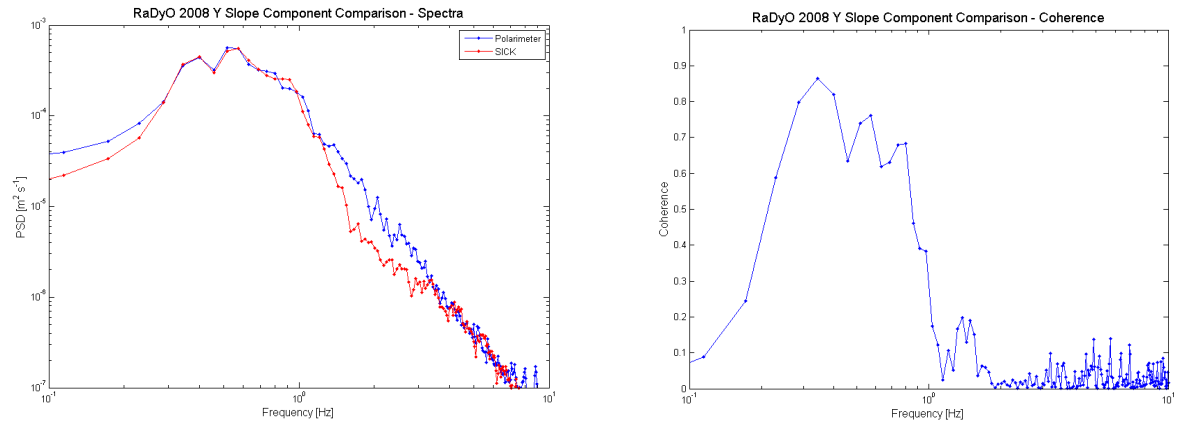

Figure 5. (Left) Comparison frequency spectra of the local wave slope over a 1 meter baseline determined from the polarimeter and scanning lidar instruments of the 20 minute records; (Right) Coherence between the slope data from the polarimeter and scanning lidar instruments. These data were taken from FLIP in approximately 5.2 m s^{-1} winds in the Santa Barbara channel during September, 2008.

Wavenumber-frequency spectrum from the polarimeter data in the wind direction show that the energy follows the deep-water dispersion relationship at wavenumbers up to roughly 100 rad m^{-1} and frequencies up to 5 Hz (Figure 6 Left). At higher wavenumbers and frequencies the wave energy diverges from the dispersion relation and suggests modulation of smaller scale waves by longer waves. Wavenumber-frequency spectrum in the cross-wind direction shows little energy at wavenumbers below 50 rad m^{-1} and 5 Hz with little detectable wave energy at higher wavenumber and frequency (Figure 6 Right).

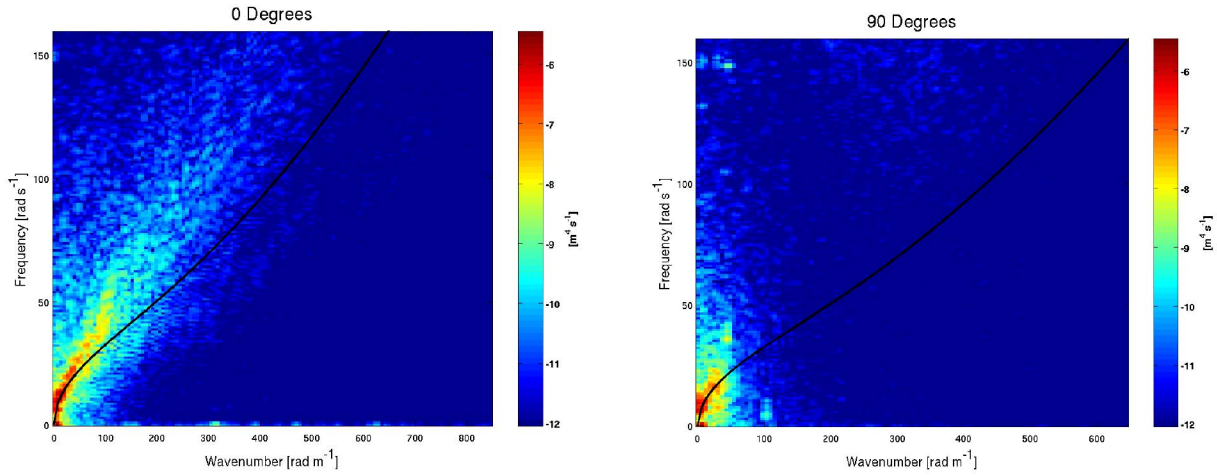

Figure 6. Wavenumber-frequency spectrum from the polarimeter data in the wind (Left) and cross-wind (Right) directions during the RaDyO Santa Barbara Channel Experiment with a wind speed of 2.0 m s^{-1}.

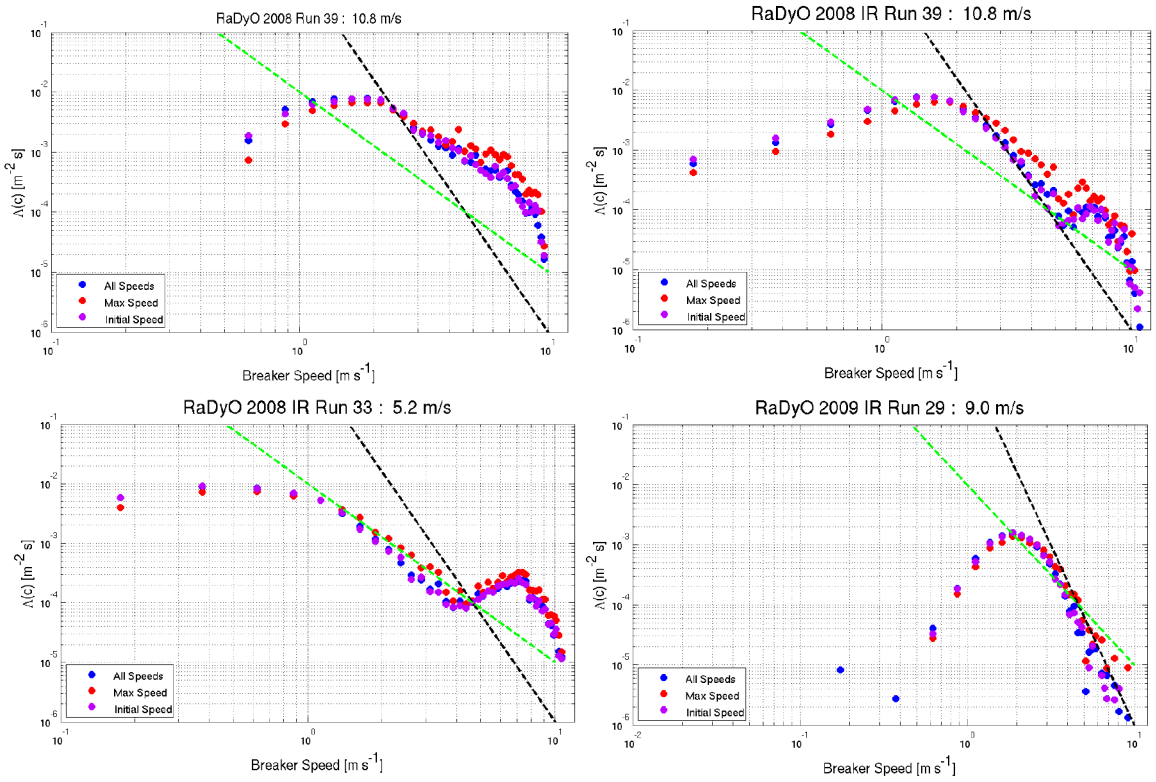

Figure 7. (Top Left) The breaking crest length distribution Λ(c), obtained by the discrete breaker tracking decomposition method for visible imagery at 10.8 m s^{-1} during RaDyO Santa Barbara Channel Experiment. (Top Right) The breaking crest length distribution Λ(c), for infrared imagery at 10.8 m s^{-1} during RaDyO Santa Barbara Channel Experiment. (Bottom Left) The breaking crest length distribution Λ(c), for infrared imagery at 5.2 m s^{-1} during RaDyO Santa Barbara Channel Experiment. (Bottom Right) The breaking crest length distribution Λ(c), for infrared imagery at 9.0 m s^{-1} during RaDyO Western Pacific Ocean Experiment off Hawaii. Dashed line is the Phillips (1985) prediction of C^{-6} behavior in the equilibrium range.

The scale of wave breaking during both field experiments aboard R/P Flip ranged from microbreakers to small-scale breakers with air entrainment to breaking dominant waves. These data will be analyzed in terms of breaking crest length density, foam coverage and whitecap persistence. Preliminary results on the breaking crest length distribution Λ(c), obtained by the discrete breaker tracking decomposition method, are shown in Figure 7 for RaDyO experiments in Santa Barbara Channel (Top Left, Top Right, and Bottom Left) and in the Western Pacific Ocean off Hawaii (Bottom Right). Figure 7 Top Left is Λ(c) from video imagery and Figure 7 Top Right is Λ(c) from infrared imagery. The comparison of Λ(c) determined from visible and infrared imagery at the same wind speed of 10 m s^{-1} show the infrared captures more of the microbreaking at smaller breaking scale and suggests that small-scale roughness is important to the breaking distribution. Figure 7 Bottom Left shows Λ(c) from infrared imagery at a wind speed of 5.2 m s^{-1}. Comparison of Λ(c) determined from the infrared

imagery at 10.8 m s^{-1} and 5.2 m s^{-1} shows more microbreaking at smaller scale at lower wind speeds suggesting that the breaking strength, *b*, varies with wind speed or microbreaking becomes less dominant with increasing wind speed. For the Santa Barbara Channel, a bimodality exists that may result from the difference in the relaxation of the young and established seas in this rapidly changing wind field. It is possibly linked to the relaxing longer seas that are sufficiently nonlinear for breaking to persist. Figure 7 Bottom Right shows $\Lambda(c)$ from the infrared imagery at a wind speed of 9.0 m s^{-1}. Small-scale wave breaking was significantly less in the Western Pacific Ocean off Hawaii than in Santa Barbara Channel. The 4 examples show the maximum distribution of breaking crests in the intermediate to short wave range with a variation in the absolute values below this range. However, the slope of the curves are close to the canonical value $\Lambda(c)\ c^{-6}$.

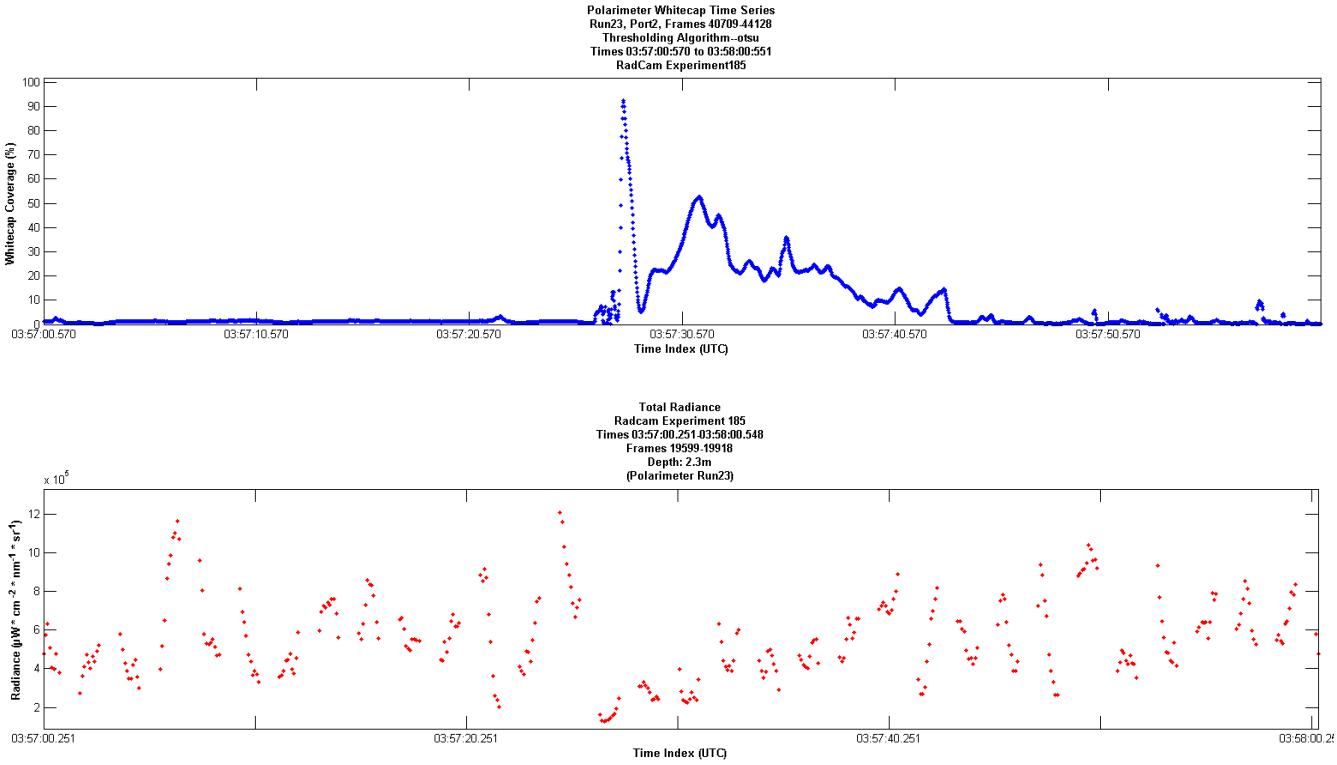

Figure 8. (Top) Time series of whitecap coverage determined from the polarimeter from a breaking event during the Western Pacific Ocean experiment off Hawaii. (Bottom) Time series of total radiance measured from the RadCam deployed directly beneath the ocean surface imaged by the polariemeter. The nominal wind speed was 9.0 m s^{-1}.

We have developed a collaboration with Marlon Lewis of Dalhousie University to link the spectral breaking crest distribution characterization to the attenuation of the light field. Figure 8 Top shows the time series of whitecap coverage determined from the polarimeter from a breaking event during the Western Pacific Ocean experiment off Hawaii in a wind speed of 9.0 m s^{-1}. Figure 8 Bottom shows the

time series of total radiance measured from the RadCam deployed directly beneath the ocean surface imaged by the polariemeter. The whitecapping fraction quickly increases during the breaking event and slowly decays to the background within 15-20 seconds. The total radiance shows the wave-like signature in response to the longer waves and then suddenly decreases sharply at the beginning of the breaking event and slowly recovers back to its initial level within 20 seconds as the whitecap fraction decreases.

IMPACT/APPLICATIONS

This effort will provide a far more detailed characterization of the wind driven air-sea interface, including wave breaking (whitecaps and microscale breaking). This is needed to provide more complete parameterizations of these processes, which will improve the accuracy of ocean optical radiative transfer models and trans-interfacial image reconstruction techniques.

RELATED PROJECTS

The results and publication here led to a DURIP award ("Equipment in Support for Polarimetric Imaging," PI: Dr. Howard Schultz, Award Number: N00014-07-1-0731) for a PSS system that will spark a new class of instrumentation that will benefit a wide variety of oceanography and fluid mechanics research and educational programs. The DURIP will contribute PSS directly towards our effort within the ONR RaDyO DRI scheduled for FY07-10 and will provide a much-needed refinement in the representation of surface wave distortion in present air-sea interfacial optical transmission models.

The work here is a direct follow-on from the Waves, Air-Sea Fluxes, Aerosols, and Bubbles (WASFAB) experiments in 2005 at the FRF pier in Duck, NC. The results from WASFAB will directly augment the capabilities for quantification of the distribution of microscale wave breaking and whitecapping in the understanding of air-sea interaction.

REFERENCES

Cox, C.S. and Munk, W.H., 1954: Measurements of the roughness of the sea surface from photographs of the sun glitter. J. Opt. Soc. Am. 44, 838-850.

Gemmrich, J.R., M.L. Banner and C. Garrett, 2008: Spectrally resolved energy dissipation and momentum flux of breaking waves. J. Phys. Oceanogr. 38, 1296-1312.

Holthuijsen, L.H., and T.H.C. Herbers, 1986: Statistics of breaking waves observed as whitecaps in the open sea, Journal of Physical Oceanography, 16, 290-297.

Jessup, A.T. and Phadnis, K.R. 2005 Measurement of the geometric and kinematic properties of microsacle breaking waves from infrared imagery using a PIV algorithm. Meas. Sci. Technol. 16, 1961-1969.

Phillips, O. M. (1985), Spectral and statistical properties of the equilibrium range in wind-generated gravity waves, *Journal of Fluid Mechanics, 156*, 505-531.

Phillips, O.M., Posner, F.L.and Hanson, J.P., 2001: High resolution radar measurements of the speed distribution of breaking events in wind-generated ocean waves: surface impulse and wave energy dissipation rates. J. Phys. Oceanogr., 31, 450–460.

Zappa, C. J., W. E. Asher, et al. (2004). "Microbreaking and the enhancement of air-water transfer velocity." Journal of Geophysical Research, **109**(C08S16): doi:10.1029/2003JC001897.

PUBLICATIONS

Christopher J. Zappa, Michael L. Banner, Howard Schultz, Andres Corrada-Emmanuel, Lawrence B. Wolff & Jacob Yalcin (2008) "Retrieval of short ocean wave slope using polarimetric imaging," Measurement Science and Technology, 19, 055503, doi: 10.1088/0957-0233/19/5/055503. [Published, Refereed]

Howard Schultz, Christopher J. Zappa, Michael L. Banner, Andres Corrada-Emmanuel and Larry Pezzaniti (2008) "A Method for Recovering the Two-dimensional slope field of the Ocean Surface Waves Using an Imaging Polarimeter," 2008 AGU Ocean Sciences Meeting, Orlando, FL March 2-7, oral presentation. [Published]